PHYSICAL REVIEW E **68**, 061201 (2003)

Partitioned density functional approach for a Lennard-Jones fluid

Shiqi Zhou*

Research Institute of Modern Statistical Mechanics, Zhuzhou Institute of Technology, Wenhua Road, Zhuzhou City, 412008, People's Republic of China

(Received 14 July 2003; published 11 December 2003)

The existing classical density functional approach for nonuniform Lennard-Jones fluid, which is based on dividing the Lennard-Jones interaction potential into a short-range, repulsive part, and a smoothly varying, long-range, attractive tail, was improved by dividing the bulk second-order direct correlation function into strongly density-depending short-range part and weakly density-depending long-range part. The latter is treated by functional perturbation expansion truncated at the lowest order whose accuracy depends on how weakly the long-range part depends on the bulk density. The former is treated by the truncated functional perturbation expansion which is rewritten in the form of the simple weighted density approximation and incorporates the omitted higher-order terms by applying Lagrangian theorem of differential calculus to the reformulated form. The two approximations are put into the density profile equation of the density functional theory formalism to predict the density distribution for Lennard-Jones fluid in contact with a hard wall or between two hard walls within the whole density range for reduced temperature $T^*=1.35$ and a density point for reduced temperature $T^*=1$. The present partitioned density functional theory performs much better than several previous density functional perturbation theory approaches and a recently proposed bridge density functional approximation.

DOI: 10.1103/PhysRevE.68.061201 PACS number(s): 61.20.Gy, 71.15.Mb

I. INTRODUCTION

Classical density functional theory (DFT) has been developed during the last two decades. Various approximations for excess Helmholtz free energy density functional $F_{ex}([\rho],T^*\cdots)$. Here, ρ stands for the density distribution, $T^*=1/\beta\varepsilon$ is the reduced temperature with $\beta=1/kT$ (k, T are Boltzmann's constant and absolute temperature respectively), and ε is the interaction strength parameter, or its functional derivative, i.e., the nonuniform first-order direct correlation function (DCF) $C^{(1)}(\mathbf{r};[\rho],T^*\cdots)$, had been proposed. However, most of these approximations is for hard sphere model fluid. For example, the weighted density type approximation [1], the functional perturbation expansion approximation [2], the fundamental measure functional [3], the bridge density functional [4], etc. For more complicated nonuniform fluid, for example, the Lennard-Jones (LJ) fluid whose potential is of the following form:

$$u_{\rm LJ}(r)=4\varepsilon\left[\left(\frac{r}{\sigma}\right)^{-12}-\left(\frac{r}{\sigma}\right)^{-6}\right]. \tag{1}$$

Here, σ is the interaction-range parameter, long-range attractive interaction has received little attention so far. Generally speaking, there are two accesses to the nonuniform LJ fluid, one is the so-called partitioning method [5] dividing the LJ interaction potential into a short-range, repulsive part, and a smoothly varying, long-range, attractive tail. The attraction is then treated in the mean field approximation (DFMFT) in which the radial distribution function $g(r;\lambda)$, where λ ($0\leqslant\lambda\leqslant1$) is a coupling parameter for the interaction potential $u_{\rm LJ}(r)$, is taken to be a Heaviside step function, or is treated by the so-called thermodynamic perturbation approximation (DFPT) which combines the density functional model of nonuniform hard sphere fluid with the Barker-Henderson second-order perturbation theory [6] extended to the nonuniform case. The other route is to treat the LJ interaction potential as a whole, this type of access can be divided into two subtypes. One is based on the bridge functional concept [7], the other is to incorporate the bulk radial distribution function into the density functional approximation [8]. As regarding the prediction accuracy for density distribution, the DFMFT is qualitatively incorrect at low densities and in significant errors at high densities. The DFPT shows a systematic improvement over the DFMFT within the whole range of liquid densities, but there is still enough room for improvement for the DFPT. Regarding the bridge density functional, it only was employed to calculate the interface structure between the LJ fluid and a wall or interface structure of the LJ fluid confined between two walls within limited density range. So it is necessary to do a detailed investigation about the bridge density functional for the LJ fluid within the whole density range, this constitutes one of the aims of the present work.

To improve the DFPT, we also will propose a DF approach based on the partitioning procedure. Instead of the above-mentioned DFMFT and DFPT, our partitioning density functional approach for Lennard-Jones fluid is based on the bulk second-order DCF. The reason for one to choose the bulk second-order DCF $C_0^{(2)}(r;\rho_b,T^*\cdots)$ ($\rho_b,T^*\cdots$ stand for the bulk parameters, ρ_b is bulk density) for the partitioning is based on the following consideration that the DCF is a functional of the interaction potential, the DCF is related to the interaction potential nonlinearly, only if one sovles the Ornstein-Zernike integral equation, then all of the nonlinearity is incorporated into the DCF. However, the DCFs are additive, it is exactly the first-order DCF that directly enters into the density profile equation. Obviously, the partitioning based on the DCF is more reasonable than that based on the interaction potential itself.

---

*Corresponding author; email address: chixiayzsq@yahoo.com

1063-651X/2003/68(6)/061201(7)/$20.00

II. DENSITY FUNCTIONAL APPROXIMATION

In DFT formalism, the density profile equation reads as follows:

$$\rho(\mathbf{r})=\rho_b \exp\{-\beta\varphi_{ext}(\mathbf{r})+C^{(1)}(\mathbf{r};[\rho],T^{*}\cdots)-C_0^{(1)}(\rho_b,T^{*}\cdots)\} \tag{2}$$

where $\varphi_{ext}(\mathbf{r})$ is the external potential responsible for generation of the density distribution $\rho(\mathbf{r})$ and $C_0^{(1)}(\rho_b,T^{*}\cdots)$ is the uniform counterpart of $C^{(1)}(\mathbf{r};[\rho],T^{*}\cdots)$.

A formal "Taylor series" expansion of the nonuniform first-order DCF $C^{(1)}(\mathbf{r};[\rho])$ around a uniform system of bulk density ρ_b can be always written down

$$C^{(1)}(\mathbf{r};[\rho],T^{*}\cdots)=C_0^{(1)}(\rho_b,T^{*}\cdots)+\int d\mathbf{r}_1(\rho(\mathbf{r}_1)-\rho_b)C_0^{(2)}(|\mathbf{r}-\mathbf{r}_1|;\rho_b,T^{*}\cdots)+\sum_{n=3}^{\infty}\frac{1}{(n-1)!}\int d\mathbf{r}_1\int d\mathbf{r}_2\cdots\int d\mathbf{r}_{n-1}\prod_{m=1}^{n-1}[\rho(\mathbf{r}_m)-\rho_b]C_0^{(n)}(\mathbf{r},\mathbf{r}_1,\cdots,\mathbf{r}_{n-1};\rho_b,T^{*}\cdots) \tag{3}$$

Here each functional derivative, i.e., the expansion coefficient $C_0^{(n)}(\mathbf{r},\mathbf{r}_1,\cdots,\mathbf{r}_{n-1};\rho_b,T^{*}\cdots)$ $n\geqslant 2$, is evaluated at the initial ρ_b. As done in a recent work [9] by the present author, when such a series is terminated, it can be an accurate representation by having the last functional derivative evaluated not at the initial ρ_b but at some $\rho_b+\lambda(\rho-\rho_b)$, with constant λ between 0 and 1 [10]. This is actually a functional counterpart of the well-known Lagrangian theorem of differential calculus which states that the following Eq. (4) is exact if the value of λ is correctly chosen. According to the above procedure, we truncated the series at the first order, then Eq. (3) reduces to

$$C^{(1)}(\mathbf{r};[\rho],T^{*}\cdots)=C_0^{(1)}(\rho_b,T^{*}\cdots)+\int d\mathbf{r}_1(\rho(\mathbf{r}_1)-\rho_b)C^{(2)}(\mathbf{r},\mathbf{r}_1;[\rho_b+\lambda(\rho-\rho_b)],T^{*}\cdots). \tag{4}$$

In the above equations, subscript 0 stands for the uniform case, its removing away corresponds to the nonuniform case. Equation (4) is exact and it does not include any approximation. It should be noted that the mixing parameter λ should be a constant value, not a field, as held by the current tendency. In fact, the functional counterpart of the Lagrangian theorem of differential calculus has been regarded as a mathematical theorem, the reader can refer to Ref. [10]. If the second-order DCF is independent of the density argument, the $C^{(2)}(\mathbf{r},\mathbf{r}_1;[\rho_b+\lambda(\rho-\rho_b)],T^{*}\cdots)$ in Eq. (4) reduces to $C_0^{(2)}(|\mathbf{r}-\mathbf{r}_1|;\rho_b,T^{*}\cdots)$.

Then Eq. (3) reduces to

$$C^{(1)}(\mathbf{r};[\rho],T^{*}\cdots)=C_0^{(1)}(\rho_b,T^{*}\cdots)+\int d\mathbf{r}_1(\rho(\mathbf{r}_1)-\rho_b)C_{0S}^{(2)}(|\mathbf{r}-\mathbf{r}_1|;\rho_b,T^{*}\cdots)+\sum_{n=3}^{\infty}\frac{1}{(n-1)!}\int d\mathbf{r}_1\int d\mathbf{r}_2\cdots\int d\mathbf{r}_{n-1}\prod_{m=1}^{n-1}[\rho(\mathbf{r}_m)-\rho_b]C_{0S}^{(n)}(\mathbf{r},\mathbf{r}_1,\cdots,\mathbf{r}_{n-1};\rho_b,T^{*}\cdots)+\int d\mathbf{r}_1(\rho(\mathbf{r}_1)-\rho_b)C_{0L}^{(2)}(\mathbf{r},\mathbf{r}_1;\rho_b,T^{*}\cdots). \tag{5}$$

Equation (5) can be rewritten as

$$C^{(1)}(\mathbf{r};[\rho],T^{*}\cdots)=C_S^{(1)}(\mathbf{r};[\rho],T^{*}\cdots)+C_L^{(1)}(\mathbf{r};[\rho],T^{*}\cdots), \tag{6}$$

where

$$C_S^{(1)}(\mathbf{r};[\rho],T^{*}\cdots)=C_{0S}^{(1)}(\rho_b,T^{*}\cdots)+\int d\mathbf{r}_1(\rho(\mathbf{r}_1)-\rho_b)C_{0S}^{(2)}(|\mathbf{r}-\mathbf{r}_1|;\rho_b,T^{*}\cdots)+\sum_{n=3}^{\infty}\frac{1}{(n-1)!}\int d\mathbf{r}_1\int d\mathbf{r}_2\cdots\int d\mathbf{r}_{n-1}\prod_{m=1}^{n-1}[\rho(\mathbf{r}_m)-\rho_b]C_{0S}^{(n)}(\mathbf{r},\mathbf{r}_1,\cdots,\mathbf{r}_{n-1};\rho_b,T^{*}\cdots) \tag{7}$$

and

$$C_L^{(1)}(\mathbf{r};[\rho],T^{*}\cdots)=C_{0L}^{(1)}(\rho_b,T^{*}\cdots)+\int d\mathbf{r}_1(\rho(\mathbf{r}_1)-\rho_b)C_{0L}^{(2)}(|\mathbf{r}-\mathbf{r}_1|;\rho_b,T^{*}\cdots). \tag{8}$$

In Eq. (5), the second and third term stand for the contribution from the density-depending part $C_{0S}^{(2)}(r;\rho_b,T^*\cdots)$ of the bulk second-order DCF to $C^{(1)}(\mathbf{r};[\rho],T^*\cdots)$, the fourth term stands for the contribution from the weakly density-depending part $C_{0L}^{(2)}(r;\rho_b,T^*\cdots)$ of the bulk second-order DCF to $C^{(1)}(\mathbf{r};[\rho],T^*\cdots)$. If the weakly density-depending part of the bulk second-order DCF is absolute, i.e., $C_{0L}^{(2)}(\mathbf{r},\mathbf{r}_1;\rho_b,T^*\cdots)$ is completely independent of the bulk density, then the fourth term is exact, the more independent is the weakly density-depending part of the bulk second-order DCF, the more accurate is the fourth term. We will give a simple proof of the argument in the Appendix. $C_{0S}^{(1)}(\rho_b,T^*\cdots)$ and $C_{0L}^{(1)}(\rho_b,T^*\cdots)$ are contributions from the density-depending part and weakly density-depending part of the bulk second-order DCF to $C_0^{(1)}(\rho_b,T^*\cdots)$. There exists the relationship $C_0^{(1)}(\rho_b,T^*\cdots)=C_{0S}^{(1)}(\rho_b,T^*\cdots)+C_{0L}^{(1)}(\rho_b,T^*\cdots)$.

Figure 1 displays the bulk second-order DCF at reduced temperature $T^*=1.35$ and several bulk densities for LJ potential truncated and shifted at $r_c^*=r_c/\sigma=4$:

$$\begin{aligned} u_{\mathrm{LJ}}^{C}(r) &= u_{\mathrm{LJ}}(r), \qquad r\leqslant r_c \\ &= 0, \qquad\qquad r\geqslant r_c . \end{aligned} \tag{9}$$

From Fig. 1, one can see that the bulk second-order DCF $C_0^{(2)}(r;\rho_b,T^*\cdots)$ is almost independent of the bulk density argument for separation distance larger than $r_{\mathrm{dcf}}=\sigma$. So we choose the $C_0^{(2)}(r;\rho_b,T^*\cdots)$ for $r\geqslant\sigma$ as $C_{0L}^{(2)}(r;\rho_b,T^*)$, then $C_0^{(2)}(r;\rho_b,T^*\cdots)$ for $r\leqslant\sigma$ is chosen as $C_{0S}^{(2)}(r;\rho_b,T^*\cdots)$. About the treatment for the contribution from $C_{0S}^{(2)}(r;\rho_b,T^*\cdots)$ to $C^{(1)}(\mathbf{r};[\rho],T^*\cdots)$, a new approach is proposed in the present paper.

The bulk second-order DCF $C_0^{(2)}(r;\rho_b,T^*\cdots)$ in Fig. 1 and that needed in the following DFT calculation are obtained by numerically sovling the Ornstein-Zernike (OZ) integral equation with the closure approximation reported in Ref. [11].

If we truncate the series in Eq. (7) at the lowest order, we arrive at

$$C_S^{(1)}(\mathbf{r};[\rho],T^*\cdots)=C_{0S}^{(1)}(\rho_b,T^*\cdots)+\int d\mathbf{r}_1(\rho(\mathbf{r}_1)-\rho_b)\times C_{0S}^{(2)}(|\mathbf{r}-\mathbf{r}_1|;\rho_b,T^*\cdots). \tag{10}$$

To display the connection between the functional perturbation expansion approximation (FPEA) and the weighted density approximation, we rewrite Eq. (10) in the form of the weighted density

$$\begin{aligned} C_S^{(1)}(\mathbf{r};[\rho],T^*\cdots) &= C_{0S}^{(1)}(\rho_b,T^*\cdots)+\int d\mathbf{r}_1(\rho(\mathbf{r}_1)-\rho_b)C_{0S}^{(2)}(|\mathbf{r}-\mathbf{r}_1|;\rho_b,T^*\cdots) \\ &= C_{0S}^{(1)}(\rho_b,T^*\cdots)+\frac{\int d\mathbf{r}_1\rho(\mathbf{r}_1)C_{0S}^{(2)}(|\mathbf{r}-\mathbf{r}_1|;\rho_b,T^*\cdots)C_{0S}^{(1)'}(\rho_b,T^*\cdots)}{C_{0S}^{(1)'}(\rho_b,T^*\cdots)}-\rho_b C_{0S}^{(1)'}(\rho_b,T^*\cdots) \\ &= C_{0S}^{(1)}(\rho_b,T^*\cdots)+C_{0S}^{(1)'}(\rho_b,T^*\cdots)(\overline{\rho}(\mathbf{r})-\rho_b), \end{aligned} \tag{11}$$

where the weighted density $\overline{\rho}(\mathbf{r})$ in Eq. (11) is exactly the one defined in the SWDA [12]

$$\overline{\rho}(\mathbf{r})=\frac{\int d\mathbf{r}'\rho(\mathbf{r}')C_{0S}^{(2)}(|\mathbf{r}-\mathbf{r}'|;\rho_b,T^*\cdots)}{C_{0S}^{(1)'}(\rho_b,T^*\cdots)} \tag{12}$$

and $C_{0S}^{(1)'}(\rho_b,T^*\cdots)=\int d\mathbf{r}C_{0S}^{(2)}(\mathbf{r};\rho_b,T^*\cdots)$ to assure the normalization of the weighting function $C_{0S}^{(2)}(r;\rho_b,T^*\cdots)/C_{0S}^{(1)'}(\rho_b,T^*\cdots)$. In the SWDA, the nonuniform first-order DCF $C^{(1)}(\mathbf{r};[\rho],T^*\cdots)$ is approximated as

$$C_S^{(1)}(\mathbf{r};[\rho],T^*\cdots)=C_{0S}^{(1)}(\overline{\rho}(\mathbf{r}),T^*\cdots). \tag{13}$$

We expand $C_{0S}^{(1)}(\overline{\rho}(\mathbf{r}),T^*\cdots)$ around the bulk density ρ_b into Taylor series, then Eq. (13) allows for the following relation:

$$\begin{aligned} C_S^{(1)}&(\mathbf{r};[\rho],T^*\cdots) \\ &= C_{0S}^{(1)}(\rho_b,T^*\cdots)+C_{0S}^{(1)'}(\rho_b,T^*\cdots)(\overline{\rho}(\mathbf{r})-\rho_b) \\ &\quad +\sum_{n=2}^{\infty}\frac{C_{0S}^{(1)^n}(\rho_b,T^*\cdots)}{n!}(\overline{\rho}(\mathbf{r})-\rho_b)^n. \end{aligned} \tag{14}$$

Comparing Eq. (11) with Eq. (14), one finds that the first-order FPEA of the $C_S^{(1)}(\mathbf{r};[\rho],T^*\cdots)$ is equal to the truncated Taylor series at first order resulting from expanding the SWDA around the bulk density ρ_b into Taylor series. Based on the similarity of Eq. (11) with the Taylor series expansion, one can make use of the Lagrangian theorem of the differ-

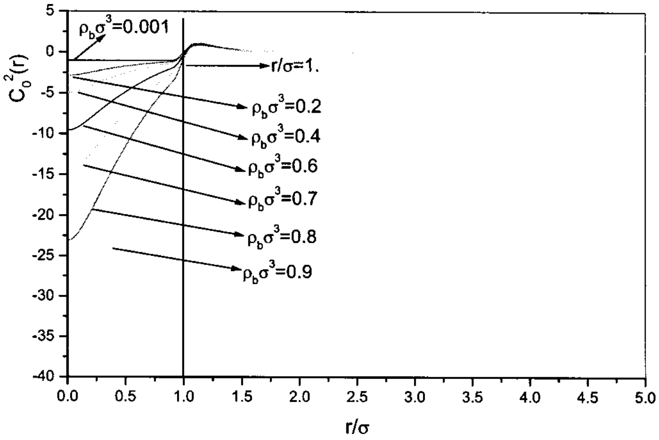

FIG. 1. The bulk second-order DCF $C_0^{(2)}(r;\rho_b,T^*\cdots)$ for several bulk densities at reduced temperature $T^*=1.35$ for the LJ potential truncated and shifted at $r_c^*=r_c/\sigma=4$.

ential calculus to incorporate the omitted terms in Eq. (11) into the lowest-order FPEA, i.e., we have

$$C_S^{(1)}(\mathbf{r};[\rho],T^*\cdots)=C_{0S}^{(1)}(\rho_b,T^*\cdots)+C_{0S}^{(1)'}(\rho_b+\lambda(\overline{\rho}-\rho_b),T^*\cdots)\times[\overline{\rho}(\mathbf{r})-\rho_b]. \tag{15}$$

Although Eq. (15) is actually the result resulting from applying the Lagrangian theorem to Eq. (14) which is based on the SWDA Eq. (13) and the Lagrangian theorem specifies the resulting adjustable parameter λ to be between 0 and 1, it is possible for the present parameter λ not to be between 0 and 1, since the SWDA is only an approximation. However, considering the nonlinear relationship between λ and $C_S^{(1)}(\mathbf{r};[\rho],T^*\cdots)$, one can expect Eq. (15) to improve on the performance of the FPEA and the SWDA. Eq. (15) was applied to the nonuniform hard sphere fluid, the predicted density profile and the surface tension are in good agreement with the corresponding simulation data [13]. Regarding the mixing parameter λ (considered as an adjustable parameter in the present approach), one can specify it following a hard wall sum rule as explained later.

Substituting Eqs. (5)–(8), and (15) into Eq. (2) leads to

$$\rho(\mathbf{r})=\rho_b\exp\left\{-\beta\varphi_{ext}(\mathbf{r})+C_{0S}^{(1)'}(\rho_b+\lambda(\overline{\rho}-\rho_b),T^*\cdots)(\overline{\rho}(\mathbf{r})-\rho_b)\int d\mathbf{r}_1(\rho(\mathbf{r}_1)-\rho_b)\times C_{0L}^{(2)}(|\mathbf{r}-\mathbf{r}_1|;\rho_b,T^*\cdots)\right\}. \tag{16}$$

The system with which we analyze the present approximations is a Lennard-Jones fluid next to a hard wall instead of the Lennard-Jones fluid in the presence of attractive walls. Since in the latter case, the attractive interaction between the fluid particle and wall may overshadow the attractive interaction between the fluid particles themselves, the former can play a more important part in determining the interface structure. The approximations for the interaction between the fluid particles are therefore difficult to evaluate clearly. The external potential in Eq. (16) therefore is of the following form

$$\beta\varphi_{\text{ext}}(z)=\infty,\quad z/\sigma<0$$
$$=0,\quad 0<z/\sigma. \tag{17}$$

We have performed computations at several bulk densities for reduced temperature $T^*=1.35$ to compare with the Monte Carlo simulation result of Balabanic *et al.* [14]. The LJ potential is truncated and shifted at $r_c=4.0\sigma$. The value of the cutoff distance r_c used in the MC simulations varied with bulk densities, but these values are estimated to be close to 4.0σ.

The mixing parameter λ was specified by a hard wall sum rule which specifies the bulk pressure P by a hard wall contact density ρ_w

$$P=\rho_w kT. \tag{18}$$

ρ_w can be obtained from $\rho(0)$ in Eq. (16) when the external potential has the same form as that in Eq. (17). The accurate pressure of bulk LJ fluid truncated and shifted at $r_c=4.0\sigma$ is difficult to obtain from available empirical equation of state. We obtain the pressure by Eq. (18) from extrapolation of the LJ-hard wall density profile to the contact point. It should be noted that the present scheme is also suitable for any external potential case other than one single hard wall case. The reason is the universality of the nonuniform first-order DCF $C^{(1)}(\mathbf{r};[\rho])$ as analyzed in detail in Ref. [9]. The calculation results are displayed in Figs. 2–4. Also, in order to investigate the performance of the bridge density functional applied to the nonuniform LJ fluid at the whole density range, we also displayed the prediction of the bridge density functional which specifies the nonuniform first order DCF by following formulas:

$$C^{(1)}(\mathbf{r};[\rho],T^*\cdots)=C_0^{(1)}(\rho_b,T^*\cdots)+\int d\mathbf{r}_1(\rho(\mathbf{r}_1)-\rho_b)\times C_0^{(2)}(|\mathbf{r}-\mathbf{r}_1|;\rho_b,T^*\cdots)+B_{VM}\left[\int d\mathbf{r}_1(\rho(\mathbf{r}_1)-\rho_b)C_0^{(2)}(|\mathbf{r}-\mathbf{r}_1|;\rho_b,T^*\cdots)\right], \tag{19}$$

where the Verlet-modified bridge function B_{VM} is from Eq. (16) in Ref. [11].

From Figs. 2–4, one can see that the bridge density functional for nonuniform LJ fluid is only comparable in accuracy with the DFMFT at supercritical temperature $T^*=1.35$, the present partitioned DFT for nonuniform LJ fluid at the same temperature achieves higher prediction accuracy even than that of the DFPT at the low, middle, and high density region, it accurately describes the formation of the vapor layer at the interface. On the other hand, the bridge

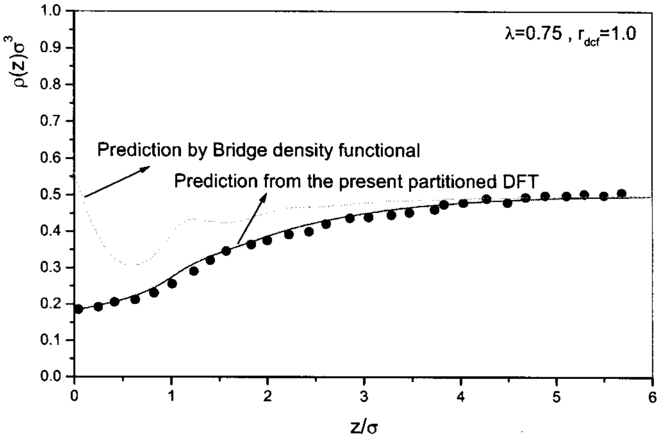

FIG. 2. Density distribution profile for a LJ fluid in contact with a hard wall at the reduced temperature $T^* = 1.35$ and the bulk density $\rho_b\sigma^3 = 0.5$ for the LJ potential truncated and shifted at $r_c^* = r_c/\sigma = 4$. The symbols are for the MC data [14], the lines are for the theoretical predictions.

density functional, as the DFMFT does, shows an oscillation in contradiction to the Monte Carlo (MC) results in the low density region. It is well-known that the bridge density functional is very accurate for the nonuniform hard sphere fluid [4,15], the bridge functional part of the bridge density functional stands for all of the terms order higher than the first order of the functional perturbation expansion of the $C^{(1)}(\mathbf{r};[\rho],T^*\cdots)$ around the bulk density. According to the above analysis, the weakly density-depending part of the bulk second-order DCF, i.e., $C_{0L}^{(2)}(r;\rho_b,T^*\cdots)$, is almost independent of the bulk density, and Eq. (8) is very accurate, the bridge functional part of the bridge density functional incurrs thus extra contribution from $C_{0L}^{(2)}(r;\rho_b,T^*\cdots)$ to $C_L^{(1)}(\mathbf{r};[\rho],T^*\cdots)$. It is exactly this unwelcomed contribution that leads to stronger oscillation than that of the MC simulation results. Since the present density functional approximation concerns an adjustable parameter λ, one can say that the good prediction is due to the adjustable parameter. In fact, if the proposed density functional approximation is intrinsically inappropriate, then only the density distribution near the hard wall is in good agreement with the simulation data. However, the present prediction for the density distribution is in better agreement with simulation data than previous DFPTs within the whole external potential range.

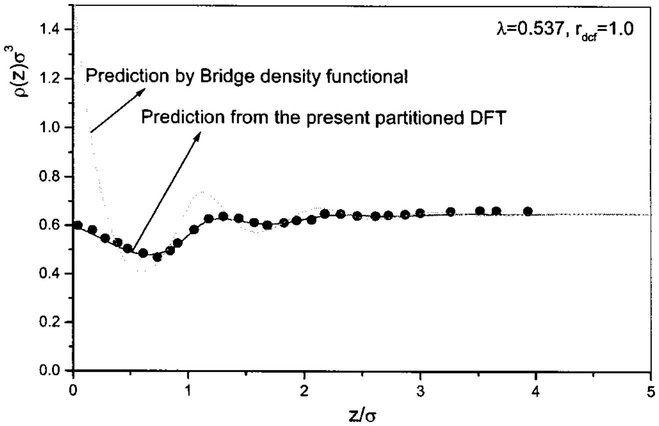

FIG. 3. Same as in Fig. 2 except that the bulk density $\rho_b\sigma^3 = 0.65$.

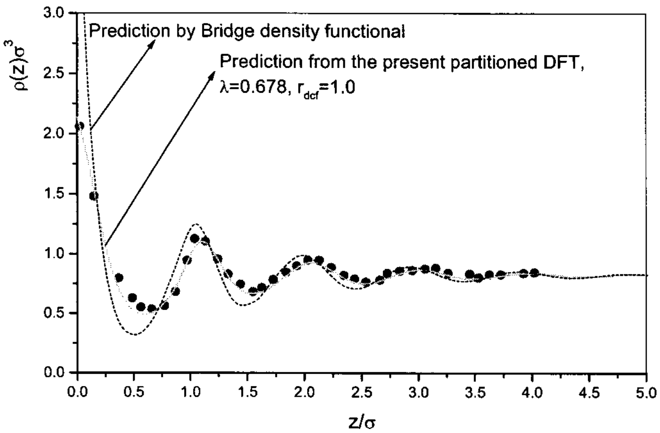

FIG. 4. Same as in Fig. 2 except that the bulk density $\rho_b\sigma^3 = 0.82$.

We also performed calculation for the density profile of LJ fluid confined by two hard walls, the external potential has the following form:

$$\beta\varphi_{\mathrm{ext}}(z) = \begin{cases} 0 & 0 < z < H\sigma \\ \infty & \text{otherwise.} \end{cases} \tag{20}$$

To compare with the recent MC simulation data [5], we calculate for the density profile generated by the external potential Eq. (20) with $H = 5$ and at bulk density $\rho_b\sigma^3 = 0.807$ and reduced temperature $T^* = 1$. For this state point, there does not exist accurate bulk pressure data, there also does not exist data for the LJ-single hard wall density profile. As a crude comparison, we specify the mixing parameter λ by equating the predicted contacting density value to the accurate MC data. Although so obtained value of λ is different from that determined by the single hard wall sum rule

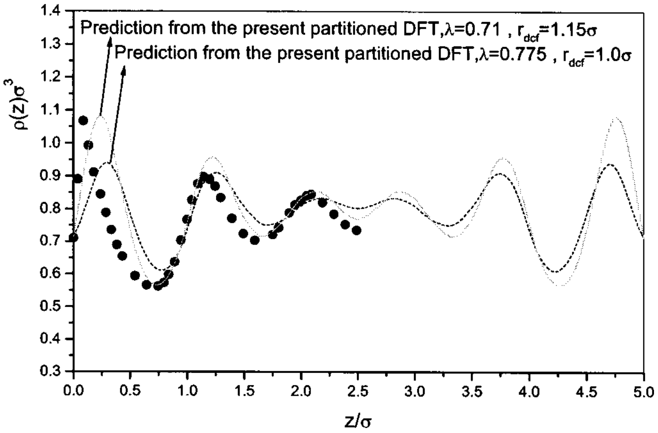

FIG. 5. Density distribution profile for a LJ fluid truncated and shifted at $r_c^* = r_c/\sigma = 2.5$ between two hard walls at the reduced temperature $T^* = 1.0$ and the bulk density $\rho_b\sigma^3 = 0.807$. The symbols are for the MC data [5], the lines are for the theoretical predictions.

due to the implicit approximation in the present density functional, we believe that the resulted difference of the density distribution profile is not significant. In Fig. 5, the predicted density profile for two cases of $r_{\mathrm{dcf}}=\sigma$ and $r_{\mathrm{dcf}}=1.15\sigma$ was displayed, near the walls the MC density profile passes through a maximum and turns download, this specular phenomena can be predicted by the present partitioned DFT, however, it cannot be described by previous DFMFT and DFPT in Ref. [5]. Furthermore the amplitude of the oscillation was exaggerated by the previous DFMFT and DFPT. It was also shown that the different cutting distance r_{dcf} can make some quantitative difference for the calculated bulk state point.

III. SUMMARY

To conclude, the present paper proposes a partitioned DFT approach based on dividing the bulk second-order DCF into density-depending part and weakly density-depending part instead of dividing the interaction potential, the contribution from the density-depending part to the first-order DCF was treated by the lowest-order FPEA which incorporates the omitted terms into itself by Lagrangian theorem of differential calculus. On the other hand, the contribution from the weakly density-depending part to the first-order DCF was treated accurately by the lowest-order FPEA. Calculation results indicate that the partitioned DFT based on dividing the bulk second-order DCF is superior to that based on dividing the interaction potential itself. The reason why the present partitioned DFT performs better is thought to be due to the functional relationship between the structure function and the interaction potential which is embodied by the nonlinear Ornstein-Zernike integral equation. So directly dividing the interaction potential is a oversimple scheme. Only by solving the nonlinear Ornstein-Zernike integral equation, all of the nonlinearity dependence on the interaction potential is embodied by the resulted bulk second-order DCF. So it is the dividing based on the bulk second-order DCF that considers the coupling between the short-range repulsive part and the long-range, attractive tail reasonably. The left problem is how to specify the critical separation distance r_{dcf}, Figure 5 shows that the choosing of the critical separation distance r_{dcf} is sometimes crucial to the final result even if the choosing is sometimes not crucial for the final result for other cases as shown in Figs. 2–4. Our calculation indicates that for the cases in Figs. 2–4, $r_{\mathrm{dcf}}=0.95\sigma$, σ, 1.15σ did not produce obvious difference for the final density distribution profile even if the final value of the adjustable parameter λ is a little different. It also should be noted that the present treatment on the contribution from the density-depending part $C_{0S}^{(2)}(r;\rho_b,T^*\cdots)$ of the bulk second-order DCF to $C_S^{(1)}(\mathbf{r};,T^*\cdots)$ is different from that reported in Ref. [9]. In Ref. [9], $C_S^{(1)}(\mathbf{r};[\rho],T^*\cdots)$ is expanded functionally around the bulk density, then the functional counterpart of the Lagrangian theorem of differential calculus was employed to make the lowest-order truncated series formally exact. However, even if the Lagrangian theorem was employed, Eq. (15) is not formally exact, because Eq. (15) is based on the simple weighted density approximation which is a crude approximation. An advantage of the present scheme for the density-depending part $C_{0S}^{(2)}(r;\rho_b,T^*\cdots)$ over that in Ref. [9] is that the calculational task is reduced.

APPENDIX

Carrying out a functional integration on the definition of the nonuniform second-order DCF with the integration path chosen as $\rho_b+\alpha(\rho-\rho_b)$

$$C^{(2)}(\mathbf{r},\mathbf{r}';[\rho],T^*\cdots)=\frac{\delta C^{(1)}(\mathbf{r};[\rho],T^*\cdots)}{\delta\rho(\mathbf{r}')} \tag{A1}$$

one obtains

$$\begin{aligned}C^{(1)}&(\mathbf{r};[\rho],T^*\cdots)\\ &=C_0^{(1)}(\rho_b,T^*\cdots)+\int_0^1 d\alpha\int d\mathbf{r}'\\ &\quad\times C^{(2)}(\mathbf{r},\mathbf{r}';[\rho_b+\alpha(\rho-\rho_b)],T^*\cdots)[\rho(\mathbf{r}')-\rho_b].\end{aligned} \tag{A2}$$

According to the spirit of the weighted density approximation, $C^{(2)}(\mathbf{r},\mathbf{r}';[\rho_b+\alpha(\rho-\rho_b)],T^*\cdots)$ can be approximated by $C_0^{(2)}(|\mathbf{r}-\mathbf{r}'|;\tilde{\rho}(\mathbf{r},\mathbf{r}';\alpha),T^*\cdots)$. Obviously if $C_0^{(2)}(r;\rho_b,T^*\cdots)$ is completely independent of the bulk density, then $C^{(2)}(\mathbf{r};\mathbf{r}';[\rho_b+\alpha(\rho-\rho_b)]T^*\cdots)$ is exactly equal to $C_0^{(2)}(r;\rho_b,T^*\cdots)$. Then Eq. (A2) reduces to Eq. (A3).

$$\begin{aligned}C^{(1)}(\mathbf{r};[\rho],T^*\cdots)=C_0^{(1)}&(\rho_b,T^*\cdots)\\ &+\int C_0^{(2)}(|\mathbf{r}-\mathbf{r}'|;\rho_b,T^*\cdots)\\ &\times[\rho(\mathbf{r}')-\rho_b]d\mathbf{r}'.\end{aligned} \tag{A3}$$

---

[1] P. Tarazona, Mol. Phys. **52**, 81 (1984); Phys. Rev. A **31**, 2672 (1985); A. Khein and N. W. Ashcroft, Phys. Rev. Lett. **78**, 3346 (1997).

[2] T. V. Ramakrishnan and M. Yussouff, Phys. Rev. B **19**, 2775 (1979); G. Rickayzen and A. Augousti, Mol. Phys. **52**, 1355 (1984); S. Zhou and E. Ruckenstein, Phys. Rev. E **61**, 2704 (2000).

[3] Y. Rosenfeld, Phys. Rev. Lett. **63**, 980 (1989); M. Schmidt, Phys. Rev. E **62**, 4976 (2000); P. Tarazona, Phys. Rev. Lett. **84**, 694 (2000).

[4] S. Zhou and E. Ruckenstein, J. Chem. Phys. **112**, 8079 (2000); S. Zhou, Phys. Rev. E **63**, 051 203 (2001); S. Zhou and X. Zhang, *ibid.* **64**, 011 112 (2001).

[5] Z. Tang, L. E. Scriven, and H. T. Davis, J. Chem. Phys. **95**, 2659 (1991); S. Varga, D. Boda, D. Henderson, and S. Sokolowski, J. Colloid Interface Sci. **227**, 223 (2000).

[6] J. S. Barker and D. Henderson, Rev. Mod. Phys. **48**, 587 (1976).

[7] S. Zhou and X. Zhang, Acta Physico-Chimica Sinica **18**(8), 699 (2002); S. Zhou, Commun. Theor. Phys. **38**, 355 (2002).

[8] S. Zhou, Phys. Rev. E **63**, 061 206 (2001); S. Zhou, J. Chem. Phys. **115**, 2212 (2001).

[9] S. Zhou, New J. Phys. **4**, 36 (June 2002).

[10] V. Volterra, *Theory of Functionals*, (New York, Dover, 1959), p. 26; in *Density-Functional Theory of Atoms and Molecules*, edited by R. G. Parr and W. Yang (Oxford University Press, New York, 1989), p. 249.

[11] N. Choudhury and S. K. Ghosh, J. Chem. Phys. **116**, 8517 (2002).

[12] S. Zhou, J. Chem. Phys. **110**, 2140 (1999).

[13] S. Zhou (unpublished).

[14] C. Balabanic, B. Borstnik, R. Milcic, A. Rubcic, and F. Sokolic, in *Static and Dynamic Properties Liquids*, edited by M. Davidovic and A. K. Soper, of Springer Proceedings in Physics Vol. 40 (Springer, Berlin, 1989), p. 70.

[15] S. Zhou, Chin. Phys. Lett. **20**, 2107 (2003).